DEVELOPMENT AND CELLULAR RESPONSE OF DIFFERENT FLUORAPATITE LAYERS ON POROUS ZIRCONIA TAPES

María P. ALBANO[a], Liliana B. GARRIDO[a], Lucas Novaes TEIXEIRA[b], Adalberto Luiz ROSA[b], Paulo TAMBASCO DE OLIVEIRA[b]

[a] Centro de Tecnología de Recursos Minerales y Cerámica (CETMIC),
M. B. Gonnet, Provincia de Buenos Aires, ARGENTINA. Fax 54 (0221) 471-0075.E-mail:palbano@cetmic.unlp.edu.ar

[b] Universidad de Sao Paulo-Facultad de Odontología de Ribeirao Preto (FORP-USP). Av. Do Café, s/n- Campus USP Monte Alegre 14040-904 Ribeirao Preto-Sao Paulo-Brasil.

ABSTRACT

Fluorapatite (FA) layers with different thickness and microstructures on porous 3 mol% yttria-partially stabilized zirconia (Y-PSZ) substrates have been fabricated by dipping porous zirconia tapes into aqueous fluorapatite slurries. Two different binders, poly(vinyl)alcohol (PVA) and latex were used to prepare the fluorapatite dip coating slips. The influence of the suspension properties and the porous structure of the tape surfaces on the layer formation rate were studied. In addition, the microstructure and the osteoblastic cellular response of the layers produced by using the different dip-coating slips were compared. The casting rate of both FA slurries at the top surface of the tapes was greater than that at the bottom surface. For each tape surface, the casting rate was accelerated and the layer shrink during sintering was reduced by using the dip coating slip with latex. The coating layer produced with latex enhanced the osteogenic potential of osteoblastic cells in vitro.

Keywords: Porous ZrO_2 tapes; Fluorapatite layers; Dip coating; Osteoblastic cell response.

1. INTRODUCTION

Calcium orthophosphates such as fluorapatite ($Ca_{10}(PO_4)_6F_2$) are widely used as bone substitute materials due to their chemical similarity to the mineral component of mammalian bones and theeth (1). The major limitations to use fluorapatite as load-bearing biomaterials is its mechanical properties, it is brittle with a poor fatigue resistance (1). Bioinert ceramic such as porous ZrO_2 can be coated with FA to achieve a high mechanical strength as well as a suitable biocompatibility of the system.

Coating layers dense and uniform with thickness of 5-20 µm retaining high chemical and thermal stability can be produced by dip coating. When a dry porous substrate is dipped into a ceramic suspension and subsequently withdrawn from it, a wet dense cake of well-defined thickness can be formed on the substrate surface. After being dried and sintered, a ceramic layer is achieved.

We have previously studied the tape casting process to produce porous zirconia substrates using starch and an acrylic latex emulsion as fugitive additive and binder, respectively (2). Besides, the processing of stable concentrated aqueous FA suspensions with the addition of ammonium polyacrylate (NH_4PA) and Poly(vinyl)alcohol (PVA) as dispersant and binder, respectively, was investigated (3). In this work, porous Y-PSZ tapes with 31.4 vol.% porosity were produced by tape casting; then, sections of these tapes were dip coated into the different concentrated aqueous FA slurries to produce FA layers.

Two mechanisms govern the formation of a layer on a porous body during dip coating. The first mechanism is known as liquid entrainment, and occurs as the plate-like specimen is withdrawn from the slurry faster than the liquid can drain from its surface, leaving a thin slurry film (4). The second mechanism is slip casting, the capillary suction caused by the porous substrate drives ceramic particles to concentrate at the substrate-suspension boundary, and a wet layer is formed (5). The withdrawal velocity of the specimen and the suspension viscosity have influence on the liquid entrainment mechanism. The microstructure of the substrate (porosity and pore diameter) together with the structure of the wet layer have influence on the slip casting mechanism. In this work, two different binders PVA and an acrylic latex emulsion were used to prepare the FA suspensions. The influence of the suspension properties and the porous structure of the tape surfaces (top and bottom) on the formation rate and consequently on the layer thickness formed on each surface were studied. In addition, the microstructure and the osteoblastic cellular response of the layers produced by using the different dip-coating slips were compared.

2. EXPERIMENTAL PROCEDURE

2.1. Raw materials and processing

A commercial 3 mol% yttria- partially stabilized zirconia doped with 0.3 wt% Al_2O_3 (Saint-Gobain ZirPro, Chine) was used to produce the cast tapes. The mean particle diameter and the specific surface area were 0.15 μm and 12.25 m^2/g, respectively. Potato starch commercially available in Argentina was used as pore former agent. The starch granules exhibit a small degree of anisotropy with a median equivalent diameter of about 50 μm.

A commercial ammonium polyacrylate (NH_4PA) solution (Duramax D 3500, Rohm & Haas, Philadelphia, PA) was used as a dispersant. The binder was an acrylic latex emulsion (Duramax B1000, Rohm & Haas, Philadelphia PA) with solids loading of 55 wt. %, an average particle size of 0.37 μm, and a glass transition temperature of -26 $^{\circ}$C.

The $Ca_3(PO_4)_2$ (Fluka, Germany) and CaF_2 (Sigma–Aldrich, Ireland) powders were mixed in stoichiometric ratio and calcined 3 hs at 1000 °C. Then, the powder was milled in an attrition mill using 1.6 mm zirconia balls with 0.047 wt% NH_4PA during 48 hours. The milled powder was washed with distilled water and dried at 100 °C. This powder subsequently referred as FA was used to prepare the suspensions for dip coating. NH_4PA was used as deflocculant and two different binders a 9 wt% PVA solution and the acrylic latex emulsion were employed to prepare the different FA suspensions.

Concentrated aqueous Y-PSZ suspensions with a solid loading of 77 wt. % were prepared by deagglomeration of the powder in distilled water with 0.3 wt.% NH_4PA (dry weight base of powder) using an ultrasonic bath. 13 wt% of starch (dry weight base of Y-PSZ powder) was added to the stabilized Y-PSZ slips followed by ultrasonic treatment. Subsequent to this, 25 wt. % latex (dry weight basis with respect to (Y-PSZ + starch) powders) was added to the slurry, followed by additional stirring. The pH of the suspensions was adjusted to 9.0 with ammonia (25 wt. %).

The Y-PSZ slips were cast manually on a Mylar film using an extensor. The gap between the extensor and the film was adjusted to 0.4 mm. The cast tapes were subsequently dried in air at room temperature up to constant weight; afterwards, they were stripped from the film and sectioned into rectangular pieces of 2.75 cm x 1.65 cm. The burn out of organic additives was achieved by slow heating (1 °C/min) up to 1000 °C. Then, the pre-calcined tapes were sintered at 1500 °C for 2 h, with a heating rate of 5 °C/min.

Aqueous FA slips with 0.6 wt% NH_4PA and different contents of the two binders: 5 wt% PVA and 15 wt% latex, were prepared by suspending particles in deionized water via 20 min of ultrasound; the pH was manually adjusted to be maintained at 9. The sintered tapes were vertically dipped into the FA suspension; after immersion during different times they were withdrawn from the suspension. All specimens were immersed and withdrawn at a constant rate of 8 mm/s. The dip-coated samples were allowed to dry at room temperature in the vertical orientation, further dried in air at 60 °C, heated for 30 min at 600 °C for binder burn out and sintered at 1200 °C for 1h.

The biological assays was carried out using Y-PSZ discs, 12 mm in diameter and 3 mm thickness, produced by slip casting and sintered at 1500 °C for 2 h; the Y-PSZ discs had nearly full density (> 98% theoretical density). The discs were then dipped into the different FA suspension for 120 s, dried and sintered as described for the coated tapes.

2.2. Characterization techniques

The viscosity of the aqueous FA slips with 0.6 wt% NH_4PA and different contents of the two binders: 5 wt% PVA and 15 wt% latex were measured. Steady state flow curves of FA slips were performed by measuring the steady shear stress value as a function of shear rate in the range of 0.5 to 542 s^{-1} using a concentric cylinder viscometer (Haake VT550, Germany) at 25 °C.

Dipped tapes were diamond polished and examined by SEM; the layer thickness on the top and bottom surfaces was measured. The microstructure of the FA coating layer after sintering produced using the different dip coating slips was observed by SEM.

2.3. Biological assays

2.3.1. Cell culture

The MC3T3-E1 cell lineage (subclone 14) was obtained from the American Type Culture Collection (ATCC) and cultured in Dulbecco's modified Eagle medium (DMEM; Gibco, Invitrogen, Grand Island, NY) supplemented with 10% fetal bovine serum (Gibco), 100 U/ml penicillin (Invitrogen) and 100 µg/ml streptomycin (Invitrogen) in 75 cm^2 flasks (Corning Incorporated, Costar, Corning, NY). The cultures were incubated at 37° C in a humidified atmosphere of 5% CO_2 and 95% air. The medium was changed every 2 or 3 days. At confluence, cells were harvested after treatment with 1 mM ethylenediamine tetraacetic acid (EDTA) (Gibco) and 0.25% trypsin (Gibco). Then, the cells were plated on the discs in 24-well polystyrene culture plates (Corning) at a cell density of 2×10^4 cells/well and cultured for up to 21 days. The cells were grown in osteogenic medium containing DMEM (Gibco) supplemented with 10% fetal bovine serum (Gibco), 100 U/ml penicillin (Invitrogen), 100 µg/ml streptomycin (Invitrogen), 5 µg/mL ascorbic acid (Gibco), and 7 mM β-glycerophosphate (Sigma, St. Louis, MO). During the culture period, cells were incubated at 37° C in a humidified atmosphere of 5% CO_2 and 95% air. The medium was changed every 2 or 3 days.

2.3.2 Cell proliferation

Cell proliferation was evaluated by 3-[4,5-dimethylthiazol-2-yl]-2,5-diphenyl tetrazolium bromide (MTT, Sigma) assay (6). At 3, 7 and 12 days, the osteoblastic cells were incubated with 10% of MTT (5 mg/ml) in culture medium at 37° C for 4 h. The medium was then aspirated from the well, and 1 ml of acid isopropanol (0.04 N HCl in isopropanol) was added to each well. The plates were then stirred on a plate shaker for 5 min, and 150 µl of this solution was transferred to a 96-well format using opaque-walled transparent-bottomed plates (Corning). The optical density was read at 570–650 nm on the plate reader (µQuanti, BioTek Instruments, Inc., Winooski, VT, EUA), and data were expressed as absorbance.

2.3.3 Matrix mineralization

At day 21, cultures grown on the discs were fixed in 10% formalin for 2 h at RT, dehydrated and stained with 2% Alizarin Red S (Sigma), pH 4.2, for 10 min. The calcium content was detected using a colorimetric method (7). Briefly, 280 µl of 10% acetic acid were added to each well and the plate was incubated at RT for 30 min under shaking. This solution was vortexed for 1 min, heated to 85º C for 10 min, and transferred to ice for 5 min. The slurry was centrifuged at 13,000 g for 15 min and 100 µl of the supernatant was mixed with 40 µl of 10% ammonium hydroxide. The optical density was read at 405 nm on the plate reader (µQuanti), and data were expressed as absorbance.

All data were expressed as means ± standard deviation. Statistical comparisons of the results were performed using the non-parametric Kruskal-Wallis test, followed by the Student-Newman-Keuls test. The level of significance was 5%.

3. RESULTS AND DISCUSSION

3.1. Fluorapatite surface coating

Two mechanisms govern the formation of a layer on a porous body during dip coating. The first mechanism is known as liquid entrainment, and ocurrs as the plate-like specimen is withdrawn from the slurry faster than the liquid can drain from its surface, leaving a thin slurry film (4). This film thickness, h, is given by:

$$h=0.94\ (\gamma/\delta\ g)^{1/2}\ Ca^{2/3} \qquad \text{(A)}$$

Ca is the capillary number given by (4):

$$Ca=\eta\ V/\gamma \qquad \text{(B)}$$

where γ is the surface tension, δ is the slurry density, g is the gravity acceleration, η is the slurry viscosity and V is the withdrawal velocity. As the liquid from the thin layer of slurry evaporates, a thin coating of ceramic particles remains on the surface of the specimen. The second mechanism is a slip-casting phenomenon and occurs because the tapes, when dipped, are slightly porous and dry. The capillary suction caused by the porous substrate drives ceramic particles to concentrate at the substrate-suspension boundary, and a wet membrane, or cake, is formed, as in the slip casting process (5). In this capillary filtration, the driving force is the capillary suction pressure caused by all the pores on the surface of the substrate. Fluid flow through the consolidated layer and into the porous body is governed by Darcy′s law, which can be integrated and simplified (assuming that the permeability of the substrate is much larger than that of the layer) to express the thickness of the wet layer,L, as a function of time, t, in the form (5):

$$L=2\ (\varepsilon_s\ \gamma\ k_m\ t/\mu\ \alpha\ R)^{1/2} \qquad (C)$$

Where ε_s is the porosity of the substrate, k_m is the permeability of the wet layer, t is the time, R is the pores radius and μ represents the dispersion liquid viscosity; α is defined as:

$$\alpha= (\varphi_m\ /\varphi_0) - 1 \qquad (D)$$

where φ_0 and φ_m are the volume fraction of the particles in the suspension and in the wet layer, respectively. During the subsequent drying and sintering process, the layer shrinks only in the direction perpendicular to the substrate, the thickness of the sintered layer, $L_{sintered}$, can be expressed as (5):

$$L_{sintered}= \beta\ L \qquad (E)$$

Where β is defined as:

$$\beta = \varphi_m / (1- \varepsilon_m) \qquad (F)$$

ε_m is the porosity of the sintered layer. Substituting Eq (C) and (F) into Eq (E) gives:

$$L_{sintered}= [2\varphi_m / (1- \varepsilon_m)]\ (\varepsilon_s\ \gamma\ k_m\ t/\mu\ \alpha\ R)^{1/2} \quad (G)$$

The layer thickness squared versus immersion time for the tapes dip coated in the FA slurries prepared with PVA and latex are shown in Figs. 1a and 1b, respectively.

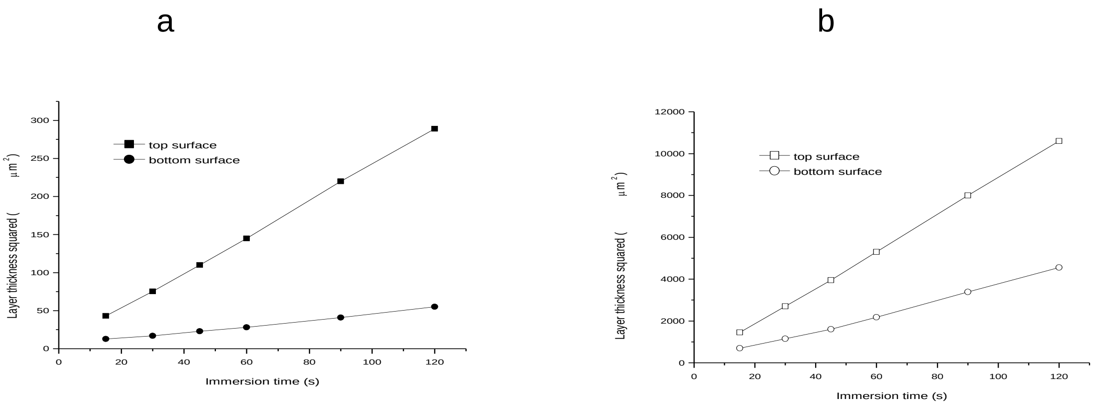

Figure 1: Layer thickness squared after sintering versus immersion time for the tapes dip coated in the FA slurries prepared with the different binders: (a) PVA; (b) latex.

Figures 2 shows the flow curves of shear stress versus shear rate at pH 9 for the different FA slips.

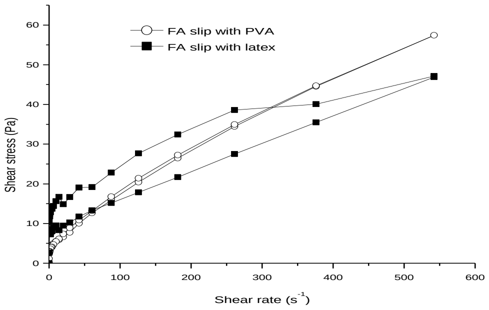

Figure 2: Flow curves of shear stress versus shear rate at pH 9 for the different FA slips.

The measured flow curves were satisfactorily fitted with the Casson model (R=0.99). The Casson model equation is:

$$\tau^{1/2}= \tau_0^{1/2}+ (\eta_p\gamma)^{1/2} \qquad \text{(H)}$$

where τ is the shear stress, γ is the shear rate, τ_0 is the yield stress and η_p represents the limiting viscosity at a high shear rate range.

Higher shear stress and viscosity values were measured for the FA slips prepared with latex with respect to those for the slips with PVA. The low τ_0 value ((τ_0=1.86 Pa) of the slip prepared with PVA indicated a weakly flocculation; while the slip with latex was strongly flocculated with an attractive network (τ_0=7.62 Pa)). The volume fraction of solids of the slip with latex and PVA was 36.2 and 27.4 vol.%, respectively. The high volume fraction of solids and τ_0 value of the slip with latex contributed to increase the slip viscosity.

The lines in Figs. 1a and 1b did not pass through the origin instead they intersected the y- vertical axis at a thickness value of about 13 and 3 μm for the slips prepared with latex and PVA, respectively. As we have previously mentioned the first mechanism in the layer formation was the liquid entrainment which leaved a thin slurry film on the tape surface (Eqs. A and B). As the viscosity values at low shear rates (0.5-1 s^{-1}) of the slips with latex were four times higher than those of the slips with PVA, a greater thickness of the film adhered, h, could be expected.

For immersion times>0, the casting rate was observed to be strongly influenced by both the structure of the tape surfaces and the suspension properties (Fig. 1).In a previous paper, the authors characterized the top and bottom surfaces of the tapes with a total bulk porosity of 31.4 vol.% and an open porosity of 16 vol.% (8). The greater porosity and the larger number of smaller pores of the top surface with respect to the bottom one increased the casting rate (Eq. C) producing thicker dip coated layers (8). A comparison of the line slopes for each tape surface (Fig. 1) indicated that the casting rate of the slip with latex was greater with respect to that with PVA, resulting in an increase of the layer thickness. As it was mentioned, the layer formation process by dip coating is similar to the formation of a cake on a porous mould by slip casting (5) in both the driving force for the liquid flow is the capillary suction pressure of the substrate. We have previously studied the casting rate of FA suspensions with different viscosities and the microstructure of the resultant green slip cast cakes (9). Our results demonstrated that the volume and size of the most frequent pore radius within the cake increased when a flocculated slip with high viscosity was cast. The greater porosity and pore size increased the permeability of the cake, thereby increasing the casting rate. Therefore, the higher casting rate of the slips with latex on both tape surfaces was attributed to the greater permeability of the wet layer (Eq. C). On the contrary for the slips with PVA, the increase in the dispersion liquid viscosity (μ) due to the water soluble PVA together with the lower permeability of the wet later (low τ_0 value), both produced a decrease in the casting rate (Eq. C).

Figure 3 shows the microstructure of the FA coating layer after sintering produced using the different dip coating slips.

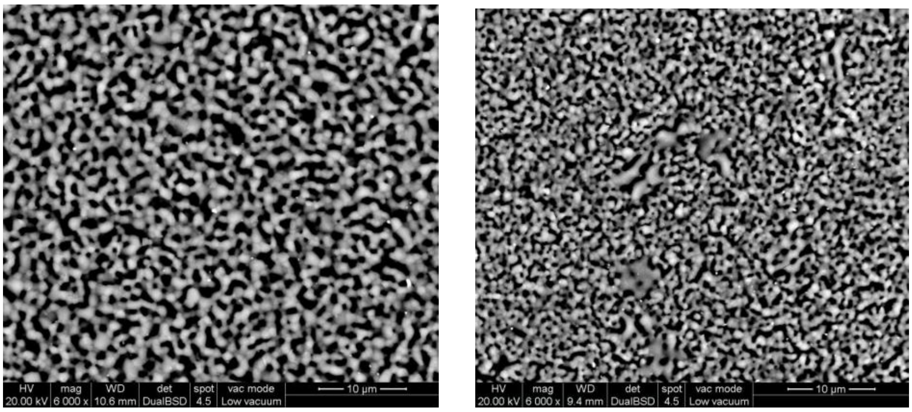

a b

Figure 3: Microstructure of the FA coating layer after sintering produced using the different dip coating slips: (a) with PVA; (b) with latex.

A greater porosity and pore size of the FA sintered layer was found when the dip coating slurry was prepared with latex. For the layer produced using the slip with latex, the coalescence of the latex particles during drying and the pore coalescence during sintering might contribute to the enlargement of the pores in the layer (8). Thus, the greater thickness of the sintered layer formed using the slip with latex for immersion times > 0 (Eq. G) was attributed to: 1) the flocculated slip which increased the permeability of the wet layer and consequently the casting rate, 2) the higher volume fraction of particles in the wet layer and 3) the more porous layer structure produced by the presence of latex.

3.2. Biological studies

The osteoblastic cell response to the control substrate and the two FA coating layers was assessed in terms of cell proliferation and matrix mineralization. Figure 4 shows the cell proliferation on the control substrate (Z) and on the coating layers produced with PVA (P) and latex (L), at 3, 7 and 12 days of culture.

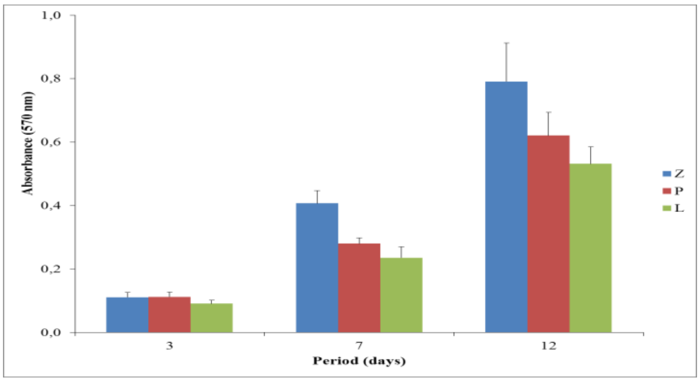

Figure 4: Cell proliferation of MC3T3-E1 cell cultures grown on the control substrate (Z) and on the coating layers produced with PVA (P) and latex (L), at 3, 7 and 12 days of culture.

For the control substrate and both coating layers, the number of cells markedly increased with the progression of cultures, confirming the favorable cell proliferation behavior. However, the (L) coating layer supported a reduced cell proliferation values compared with (Z) and (P). It is known that the physical properties of the coating layer such as porosity, roughness and morphology affect cell adhesion, spreading and proliferation (10). The less porous surface of the (P) coating layer (Fig. 3) appeared to be favorable for the cell proliferation compared with the more porous surface of the (L) coating layer. However, considering the osteoblast differentiation sequence, the acquisition of a mature, mineralized matrix-producing phenotype depends on the terminal cell cycle arrest (10), indicating that the porous surface of the (L) coating would be better to promote the osteoblast differentiation. Figure 5 shows the matrix mineralization of cultures grown on the control substrate (Z) and on the (P) and (L) coating layers at 21 days. The cells on the (L) coating layer exhibited a significantly higher mineralization (greater Ca content) compared with (Z) and (P), corroborating the results on cell proliferation. It is generally agreed that micron- and/or nanoporous material surfaces enhance bone matrix production at the material/tissue interface in vitro and in vivo (10).

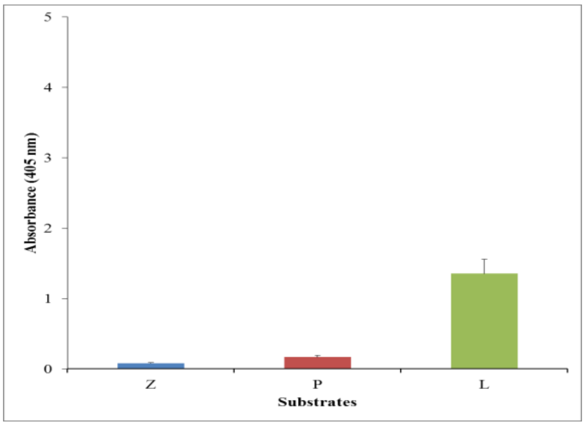

Figure 5: Matrix mineralization (Ca content) of MC3T3-E1 cell cultures grown on the control substrate (Z) and on the (P) and (L) coating layers after culturing for 21 days.

4. CONCLUSIONS

Fluorapatite layers with different thickness and microstructures on porous Y-PSZ substrates have been fabricated by dipping porous zirconia tapes into aqueous fluorapatite slurries. Two different binders, PVA and latex were used to prepare the fluorapatite dip coating slips.

A greater initial thickness of the layer adhered was found for the tapes dip coated in the FA slip with latex; for immersion times>0, the casting rate was observed to be strongly influenced by both the structure of the tape surfaces and the suspension properties. For both FA slurries, the casting rate at the top surface of the tapes was greater than that at the bottom surface. For each tape surface, the higher casting rate of the slip with latex was attributed to the greater permeability of the wet layer. Besides, the higher volume fraction of particles in the wet layer and the larger pores in the layer produced by the presence of latex also contributed to increase the thickness of the sintered layer. The less porous surface of the (P) coating layer appeared to be favorable for the cell proliferation compared with the more porous surface of the (L) coating layer. However, the (L) coating layer enhanced the osteogenic differentiation and consequently the mineralized matrix production by osteoblastic cells.

REFERENCES

(1) Weiner, S.; Wagner, H. D. The material bone: structure- mechanical function relations. Ann. Rev. Mater. Sci., v. 28, p. 271-298, 1998.

(2) Albano, M. P.; Genova, L.; Garrido, L. B.; Plucknett, K. Processing of porous yttria-stabilized zirconia by tape-casting. Ceramics International, v. 34, p. 1983-1988, 2008.

(3) Albano, M. P.; Garrido, L. B. Rheological properties of concentrated aqueous fluorapatite suspensions. Ceramics Internacional, v. 36, p. 1779-1786, 2010.

(4) Pontin, M. G.; Lange, F. F.; Sánchez-Herencia, A. J.; Moreno, R. Effect of unfired tape porosity on surface film formation by dip coating. J. Am. Ceram. Soc., v. 88, n. 10, p. 2945-2948, 2005.

(5) Gu, Y.; Meng, G. A model for ceramic membrane formation by dip-coating. J. Eur. Ceram. Soc., v. 19, p. 1961-1966,1999.

(6) Mosmann, T. Rapid colorimetric assay for cellular growth and survival: application to proliferation and cytotoxicity assays. J. Immunol. Methods, v. 65, p. 55-63, 1983.

(7) Gregory, C. A.; Gunn, W. G.; Peister, A.; Prockop, D. J. An alizarin red-based assay of mineralization by adherent cells in culture: comparison with cetylpyridinium chloride extraction. Anal. Biochem.,v. 329, p. 77-84, 2004.

(8) Albano, M. P.; Garrido, L. B. Effect of zirconia tape porosity on fluorapatite film formation by dip coating. Ceramics International, v. 39, n. 1,p. 29-37, 2013.

(9) Albano, M. P.; Garrido, L. B. Processing of concentrated aqueous fluorapatite suspensions by slip casting. J. Mater. Sci., v. 46, n. 15, p. 5117-5128, 2011.

(10) Stein, GS.; Lian, JB. Molecular mechanisms mediating proliferation/differentiation interrelationships during progressive development of the osteoblast phenotype. Endocr Rev., v. 14, n. 4, p. 424-442, 1993.